Journal of ELECTRONIC MATERIALS, Vol. 41, No. 6, 2012
DOI: 10.1007/s11664-011-1853-0

Bloating in $(Pb_{0.95}Sn_{0.05}Te)_{0.92}(PbS)_{0.08}$-0.055%$PbI_2$ Thermoelectric Specimens as a Result of Processing Conditions

JENNIFER E. NI,[1] ELDON D. CASE,[1,3] RYAN STEWART,[1] CHUN-I. WU,[1] TIMOTHY P. HOGAN,[1] and MERCOURI G. KANATZIDIS[2]

1.—Chemical Engineering and Materials Science Department, Michigan State University, Room 2527 Engineering Building, East Lansing, MI 48824-1226, USA. 2.—Northwestern University, Evanston, IL, USA. 3.—e-mail: casee@egr.msu.edu

Lead chalcogenides such as $(Pb_{0.95}Sn_{0.05}Te)_{0.92}(PbS)_{0.08}$-0.055%$PbI_2$ have received attention due to their encouraging thermoelectric properties. For the hot pressing (HP) and pulsed electric current sintering (PECS) techniques used in this study, decomposition reactions can generate porosity (bloating). Porosity in turn can degrade electrical, thermal, and mechanical properties. In this study, microstructural observations (scanning electron microscopy) and room-temperature elasticity measurements (resonant ultrasound spectroscopy) were used to characterize bloating generated during post-densification anneals. Although every HP specimen bloated during post-densification annealing, no bloating was observed for the PECS specimens processed from dry milled only powders. The lack of bloating for the annealed PECS specimens may be related to the electrical discharge intrinsic in the PECS process, which reportedly cleans the powder particle surfaces during densification.

Key words: Thermoelectrics, porosity, Young's modulus, resonant ultrasound spectroscopy

INTRODUCTION

Powder processing of thermoelectric materials can yield specimens with much smaller grain sizes than cast specimens.[1] Reduction in grain size can in turn greatly enhance the fracture strength of brittle materials.[1,2] During powder processing, porosity, P, can result from (1) incomplete sintering[2] or (2) gas evolution within the specimen during processing. Internal gas evolution in specimens during processing can occur via either liquid-phase[3,4] or solid-phase decomposition reactions.[5–9]

Solid-phase decomposition reactions[5–9] may occur when the specimen is densified using high externally applied pressures. High-temperature anneals in the absence of externally applied pressure can result in increases in P with increasing temperature due to local deformation caused by pressure generated by gases evolved by decomposition reactions. Thus in this study, the volume fraction porosity P is given by $P = P_R + P_B$, where P_R is the porosity contribution due to residual pores and P_B is the porosity generated by bloating.

The dependence of thermal, electrical, and mechanical properties on porosity, P, can be written as

$$A(P) = A_D \exp(-b_{PA}P), \quad (1)$$

where A can be thermal conductivity,[10] electrical conductivity,[10] dielectric constant,[11] or elastic modulus.[10,12] A_D is the value of the material property, A, at $P = 0$. Also, b_{PA} is a material-dependent constant,[10,12] and $P = P_R + P_B$. This study focuses on microstructural observations of bloating-generated porosity and measurements of P versus Young's modulus, E, especially where P is generated by bloating for $Ag_{0.86}Pb_{19}Sb_{1.0}Te_{20}$ (LAST) and $(Pb_{0.95}Sn_{0.05}Te)_{0.92}(PbS)_{0.08}$-0.055%$PbI_2$ (PbTe-PbS)[13] specimens.

(Received July 11, 2011; accepted December 1, 2011; published online December 22, 2011)

For both hot pressing (HP) and pulsed electric current sintering (PECS), the powder charge is placed between two movable plungers within a cylindrical die. Also, for both HP and PECS, the powder charge is heated while pressure is simultaneously applied via the plungers. However, HP and PECS are distinct powder processing techniques in that for HP the powders and die are heated by an external furnace while for PECS the powders are heated by high-current electrical pulses that pass through both the die assembly (plungers plus die) and the enclosed powder charge. Regardless of the powder processing technique used, our HP specimens bloated after annealing while specimens that were PECS processed from dry milled only powders did not bloat upon annealing ("Results and Discussion" section). During densification, gas-phase generation from decomposition reactions can be inhibited by applying elevated pressures due to hot pressing (HP) and pulsed electric current sintering (PECS). However, during post-densification thermal annealing (in the absence of externally applied confining pressure), decomposition reactions can generate porosity (bloating), which in turn can degrade electrical, thermal, and mechanical properties.[10–12,14] Changes in thermal and electrical conductivity are extremely important, since the efficiency of a thermoelectric device is a function of the dimensionless figure of merit, ZT, which is written as

$$ZT = \frac{\sigma S^2}{\kappa}, \qquad (2)$$

where σ is the electrical conductivity, S is the Seebeck coefficient, κ is the thermal conductivity, and T is temperature.

Since κ decreases with increasing porosity,[10,14] low thermal conductivity is required for high ZT for thermoelectric materials (Eq. 2). However, the electrical conductivity, σ, also decreases with increasing porosity.[10] Thus, one must consider the overall effect of porosity on ZT to determine whether increasing porosity enhances or degrades the thermoelectric properties of a material.

Calculations of the effect of nanopores on the thermal conductivity of Ge[15] and Si[16] indicate dramatic decreases in κ with nanoporosity. For nanoporous Ge with pore diameter of 1.0 nm and pore spacing of 0.7 nm, the calculated κ was 180 times smaller than the bulk value.[15] Similar decreases in κ were calculated for Si,[16] but as was the case for Ge,[15] the decreases in κ become large only for extremely high values of volume fraction porosity, P ($P \approx 0.64$ to 0.89).[16] However, ZT may decrease with increasing nanoporosity, as noted by Lee et al.,[14] who state that "Porous nanograined materials have enhanced Seebeck coefficient due to energy filtering effect and low thermal conductivity, which are favorable for thermoelectric applications. However, the benefit is not large enough to overcome the deficit in the electrical conductivity, so that a high sample density is necessary for nanograined SiGe."[14] Thus, bloating-generated porosity may degrade both ZT and mechanical properties.

EXPERIMENTAL PROCEDURES

Specimens were densified by HP or PECS of $Ag_{0.86}Pb_{19}Sb_{1.0}Te_{20}$ and $(Pb_{0.95}Sn_{0.05}Te)_{0.92}(PbS)_{0.08}$-0.055%$PbI_2$ powders that were (i) crushed, ground, sieved, and reground (CGSR), (ii) dry milled (DM), (iii) wet milled (WM) with hexane, or (iv) dry and then wet milled with hexane (D/WM) (Table I). A 53-μm sieve (Retsch, Newtown, PA) was used for each powder processing technique in this study (Table I). The hot pressed and PECS specimens were pressed using the temperature–pressure–time profiles presented in Table I with a 22-mm-diameter graphite die. In this study, two separate sets of specimens were used to (i) directly examine the microstructure of fracture surfaces using scanning electron microscopy (SEM), and (ii) nondestructively measure the porosity-dependent Young's modulus using resonant ultrasound spectroscopy (RUS) analysis (Table I). Four SEM specimens were annealed at temperatures ranging from 693 K to 973 K (Table I), and one SEM specimen was annealed successively at 663 K, 823 K, and 936 K (Table I). The nine RUS specimens were successively annealed at temperatures ranging from 543 K to 773 K (Table I). Details of the RUS experimental procedure are given elsewhere.[12]

RESULTS AND DISCUSSION

Using planetary milled powders, the mean grain sizes of the as-densified $Pb_{0.95}Sn_{0.05}Te)_{0.92}(PbS)_{0.08}$-0.055%$PbI_2$ specimens were 1 μm to 10 μm for both HP and PECS processing.[12,17] The mean grain size for the HP as-densified specimen was 20 μm when starting from CGSR powders. Both HP and PECS produced specimens that ranged in density from about 0.92 to 0.97 with spherical or quasispherical pores at grain boundaries and triple points, with submicron to 3-μm-diameter pore sizes (Figs. 1–3).

However, upon annealing, bloating occurred (Figs. 1, 2) for the as-densified HP specimens processed from powder subjected to (i) CGSR (Fig. 1d), (ii) DM (Fig. 1b), and (iii) D/WM (Fig. 2b). The as-densified PECS specimens processed from WM powders bloated (Fig. 2d). Bloating in both the HP and PECS specimens generated spherical or quasispherical pores along grain boundaries with pore diameters ranging from 1 μm to 20 μm (Figs. 1, 2). Also, the PECS PbTe-PbS WM (Fig. 2d) and HP LAST CGSR (Fig. 1d), specimens had lenticular pores from 10 μm in length and 1 μm wide to about 30 μm in length and 5μm wide.

After annealing from 2 h to 6 h at temperatures from 693 K to 973 K (Table I), the areal number density of pores increased by 10- to 30-fold compared with the pore areal density on fracture surfaces of as-densified HP specimens made from powder processed by CGSR (Fig. 1d), DM (Fig. 1b),

Table I. Powder processing conditions and sintering parameters for the hot pressed (HP) and pulsed electric current sintering (PECS) densified specimens processed using powders that were crushed, ground, sieved, and reground (CGSR). Powder was either (1) set aside for densification, (2) dry milled (DM), (3) dry milled and then wet milled (D/WM), or (4) wet milled (WM)

Specimen (Composition)	Powder Processing	Sintering, Max. Temperature/Pressure/Time	Post-densification Annealing Parameters	
			Temperature	Time
Bloating observed via SEM				
HP-DM-01[a]	DM	673 K/74.4 MPa/90 min	723 K	4 h[b]
HP-CGSR-01[a]	CGSR	673 K/74.4 MPa/90 min	973 K	6 h[b]
HP-D/WM-01	D/WM[c]	673 K/74.4 MPa/90 min	693 K	2 h[b]
PECS-WM-01	WM[d]	823 K/60 MPa/20 min	823 K	2 h[e]
PECS-DM-01	DM	823 K/60 MPa/20 min	663 K, 823 K, 936 K	2 h[e]
Bloating measured via RUS elasticity measurements				
HP-D/WM-02[a]	D/WM[c]	723 K/74.4 MPa/120 min	603 K, 633 K, 663 K, 693 K	1 min[e]
HP-D/WM-02[b]	D/WM[c]	723 K/74.4 MPa/120 min	543 K, 573 K, 603 K, 633 K, 663 K, 693 K	1 min[e]
HP-D/WM-02[c]	D/WM[c]	723 K/74.4 MPa/120 min	603 K, 633 K, 663 K, 693 K	1 min[e]
HP-D/WM-01[a]	D/WM[c]	723 K/74.4 MPa/120 min	603 K, 633 K, 663 K, 693 K	1 min[e]
HP-D/WM-01[b]	D/WM[c]	723 K/74.4 MPa/120 min	663 K, 693 K	1 min[e]
HP-WM-01[a]	WM[d]	723 K/74.4 MPa/120 min	663 K, 693 K	1 min[e]
HP-WM-01[b]	WM[d]	723 K/74.4 MPa/120 min	603 K, 633 K, 663 K, 693 K	1 min[e]
PECS-D/WM-01	D/WM[c]	823 K/60 MPa/20 min	603 K, 633 K, 663 K, 693 K	1 min[e]
PECS-DM-02	DM	623 K/60 MPa/20 min	773 K	1 min[e]

For the post-densification anneals, the heating and cooling rates were 5 K/min and 2 K/min for specimens prepared for SEM observation and RUS elasticity measurements, respectively;
[a]Specimen composition is $Ag_{0.86}Pb_{19}Sb_{1.0}Te_{20}$; all other specimens in the table are $(Pb_{0.95}Sn_{0.05}Te)_{0.92}(PbS)_{0.08}$-0.055%$PbI_2$; [b]Annealed in flowing Ar atmosphere; [c]Wet milled with hexane as milling fluid; [d]Wet milled with ethanol as milling fluid; [e]Annealed in flowing Ar (96%)–H_2(4%) atmosphere.

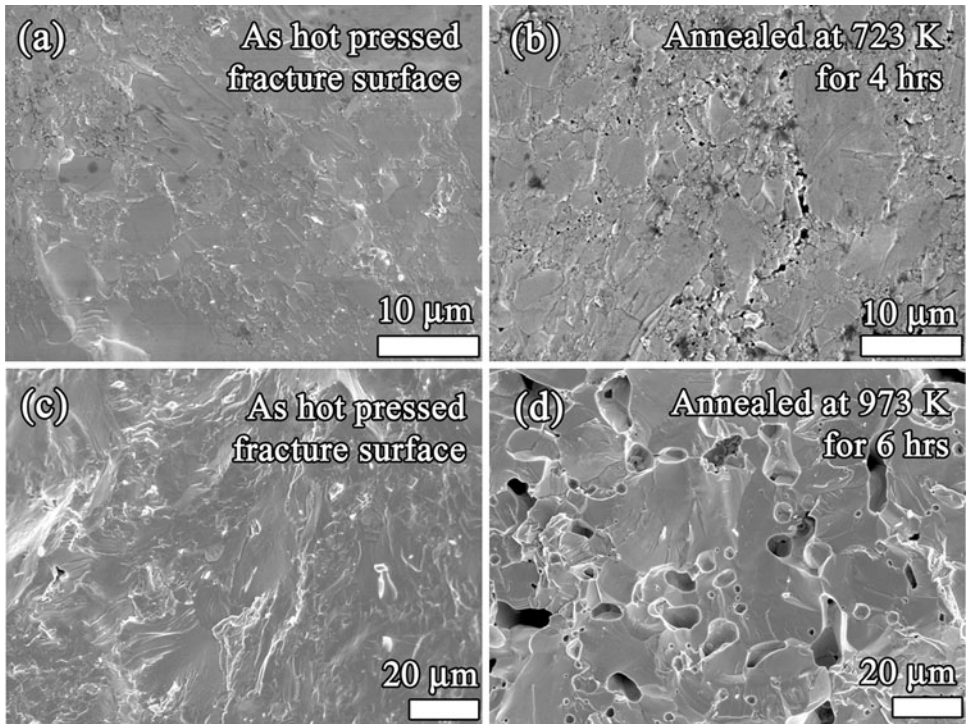

Fig. 1. As-densified fracture surfaces of (a) HP-DM-01 and (c) HP-CGSR-01 do not show bloating. Annealing (b) HP-DM-01 at 723 K for 4 h and (d) HP-CGSR-01 at 973 K for 6 h resulted in bloating, as evidenced by increased porosity of internal fracture surfaces. All annealing was performed in flowing Ar.

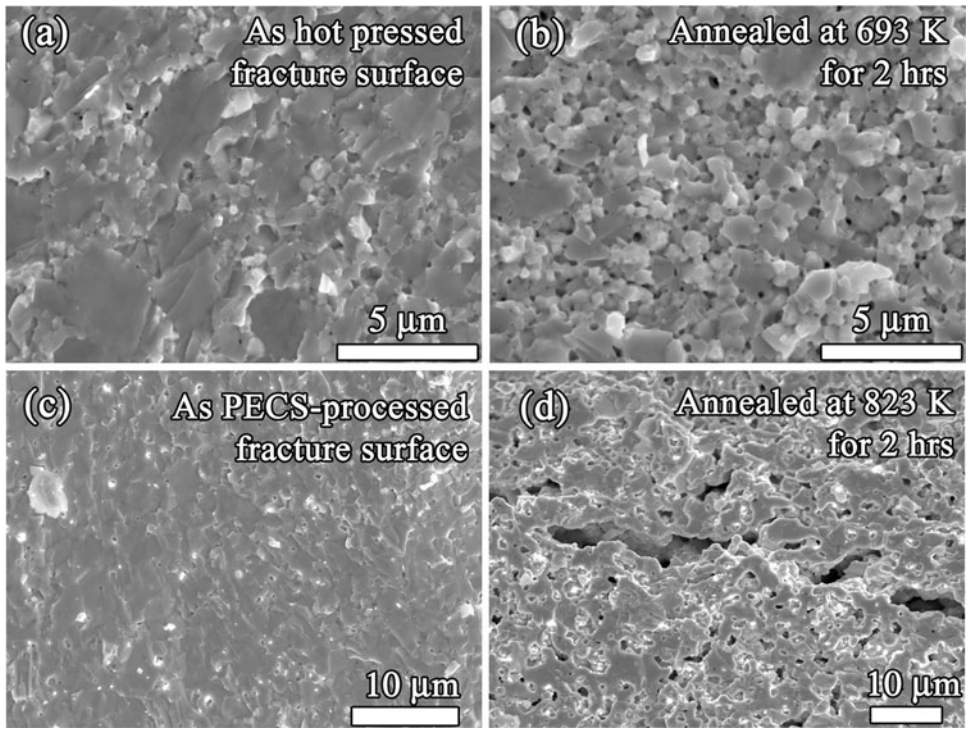

Fig. 2. As-densified fracture surfaces of (a) HP-D/WM-01 and (c) PECS-WM-01 do not show bloating. Annealing (b) HP-D/WM-01 at 693 K for 2 h and (d) PECS-WM-01 at 823 K for 2 h resulted in bloating, as evidenced by increased porosity of internal fracture surfaces. All annealing was performed in flowing Ar or Ar (96%)-H_2 (4%).

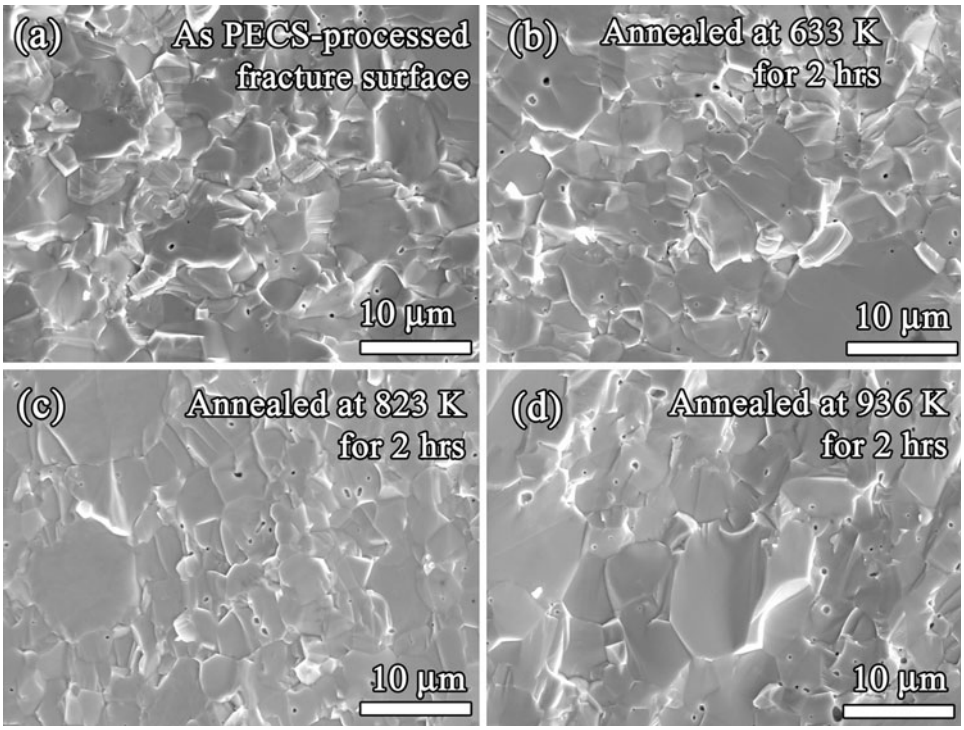

Fig. 3. In contrast to the annealing behavior depicted in Figs. 1 and 2, the (a) as-densified PECS-DM-02 did not bloat after annealing at (b) 663 K for 2 h, (c) 823 K for 2 h, or (d) 936 K for 2 h. All annealing was performed in flowing Ar (96%)–H_2 (4%).

and D/WM (Fig. 2b), and PECS specimens made from powder processed by WM (Fig. 2d). The series of anneals from 543 K to 693 K on hot pressed specimen HP-D/WM-02b (Table I) induced surface blistering that ranged from 0.5 mm to 1 mm in diameter and internal porosity that consisted of six lenticular pores per 12,000 μm^2 that were about 20 μm long and 5 μm wide. In contrast, the PECS densified specimens fabricated using DM powders did not bloat (Fig. 3) or blister when annealed for 2 h at 663 K, 823 K, and 936 K (Table I).

For the nine as-densified RUS specimens, the mass and volume were measured before and after each post-densification anneal to monitor the change in density. Before post-densification annealing, $P = P_R$, where P_R ranged from 0.03 to 0.08. Following post-densification anneals, P_B increased as temperature increased; for example, after the 603 K post-densification anneal, P ranged from 0.04 to 0.11, whereas after the 693 K anneal, P ranged from 0.05 to 0.22 (Fig. 4). On RUS analysis, the exception was the PECS-DM-02 specimen, which did not bloat after a series of anneals, including a 773 K post-densification anneal (Fig. 4; Table I). The decrease in Young's modulus, E, with increasing porosity is consistent with Eq. 1 (Fig. 4), where the least-squares fit of E versus P (Eq. 1) yielded $r^2 = 0.990$, $b_{PE} = 1.33 \pm 0.02$, and $E_D = 56.17 \pm 0.13$ GPa for the 9 as-densified and 32 post-densification annealed elastic moduli measurements.

To compare the value of the Young's modulus, E_D, found from Eq. 1 with literature, we can use values

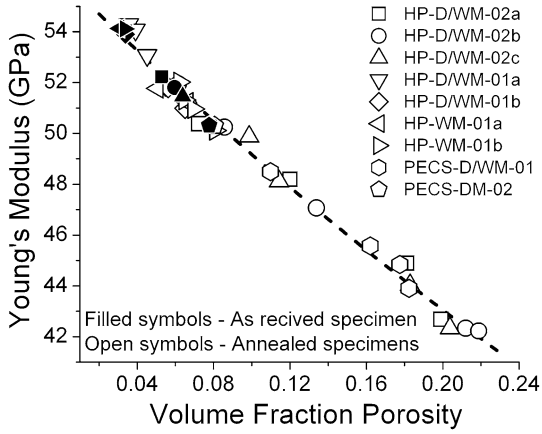

Fig. 4. The bloating (Figs. 1, 2) or lack of bloating (Fig. 3) observed on SEM study is also evident in RUS measurements of Young's modulus, E, versus volume fraction porosity, P. For the 9 as-densified HP and PECS specimens along with the 32 annealing measurements on the same 9 specimens (Table 1), as P increased, E decreased. Filled and open symbols represent E values for as-densified and annealed specimens, respectively. Equation 1, widely used to describe the E versus P behavior for brittle materials,[10,11] also fits the E versus P behavior well ($r^2 = 0.990$) for the 41 RUS measurements included in this study. The dashed line represents the least-squares fit to Eq. 1.

of the aggregate Young's modulus calculated from single-crystal PbTe data, where E was 58.08 GPa[18] or 56.95 GPa.[19] Thus, the E_D value of 56.17 $\pm$ 0.13 GPa calculated from the least-squares fit of Eq. 1 to this study's modulus-porosity data for

$(Pb_{0.95}Sn_{0.05}Te)_{0.92}(PbS)_{0.08}$-0.055%$PbI_2$ specimens is within approximately 2% of the mean of the two literature values for PbTe[18,19] listed above.

Groza et al. found that the electrical discharge that is intrinsic to the PECS process cleaned the oxide surface layers from the AlN particles during sintering.[20] In this study, the PECS densification process may have removed contaminating surface layers from the powder processed $(Pb_{0.95}Sn_{0.05}Te)_{0.92}(PbS)_{0.08}$-0.055%$PbI_2$ particles. This surface cleaning may have in turn removed the source of a solid-phase decomposition reaction, thus allowing the densified PECS specimens to be annealed up to 936 K without bloating (Table I; Fig. 3). Although the dry milled PECS specimens did not bloat (Fig. 3), in contrast the wet milled PECS specimens did bloat during post-densification anneals (Fig. 2d). Perhaps the hexane or ethanol used during the wet milling (Table I footnotes) left a carbonaceous residue which was not entirely removed by the PECS process. Such a residue could decompose during post-densification annealing, causing bloating (Fig. 2d).

CONCLUSIONS

As-densified specimens fabricated by both PECS and HP for each of four powder processing modes (CGSR, DM, WM, and D/WM) gave dense specimens with spherical porosity confined to grain boundaries. Post-densification anneals resulted in bloating (P increased) for all HP specimens. For PECS fabrication, bloating occurred for the specimens processed with WM and D/WM powders. Only the PECS DM specimens did not bloat upon annealing, perhaps due to intrinsic cleaning of powder particle surfaces during sintering.[20]

ACKNOWLEDGMENTS

This research was supported by the Office of Naval Research, Grant N00014-08-1-0613 and the Department of Energy, "Revolutionary Materials for Solid State Energy Conversion Center," an Energy Frontiers Research Center funded by the US Department of Energy, Office of Basic Energy Sciences under Award Number DE-SC0001054. Ed Timm of the Mechanical Engineering Department, Michigan State University assisted the authors with hot pressing and cutting the specimens.

REFERENCES

1. F. Ren, E.D. Case, E.J. Timm, M.D. Jacobs, and H.J. Schock, *Philos. Mag. Lett.* 86, 673 (2006).
2. M.W. Barsoum, *Fundamentals of Ceramics*, ed. B. Cantor and M.J. Goringe (London: IOP Publishing, 2003).
3. N.M.P. Low, *J. Mater. Sci.* 16, 800 (1981).
4. P. Colombo, *Philos. Trans. R. Soc. A* 364, 109 (2006).
5. D. Holz, S. Wu, S. Scheppokat, N. Claussen, and J. Am, *Ceram. Soc.* 77, 2509 (1994).
6. M.H. O'Brien, O. Hunter Jr., and E.D. Case, *J. Mater. Sci. Lett.* 4, 367 (1985).
7. H. Wen, Y. Zhao, Z. Zhang, O. Ertorer, S. Dong, and E.J. Lavernia, *J. Mater. Sci.* 46, 3006 (2011).
8. V.N. Antsiferov, V.B. Kul'met'eva, S.E. Porozova, B.L. Krasnyi, V.P. Tarasovskii, and A.B. Krasnyi, *Russ. J. Non-Ferr. Met.* 51, 82 (2010).
9. L. Stoch, *J. Therm. Anal.* 37, 1415 (1991).
10. R.W. Rice, *Porosity of Ceramics* (New York: Marcel Dekker, 1998).
11. T.P. Hoepfner and E.D. Case, *Ceram. Int.* 29, 699 (2003).
12. J.E. Ni, F. Ren, E.D. Case, and E.J. Timm, *Mater. Chem. Phys.* 118, 459 (2009).
13. J. Androulakis, C.-H. Lin, H.-J. Kong, C. Uher, Wu C-I, T. Hogan, B.A. Cook, T. Caillat, K.M. Paraskevopoulos, and M.G. Kanatzidis, *J. Am. Chem. Soc.* 129, 9780 (2007).
14. H. Lee, D. Vashaee, Z. Wang, M.S. Dresselhaus, Z.F. Ren, and G. Chen, *J. Appl. Phys.* 107, 094308 (2010).
15. J.H. Lee and J.C. Grossman, *Appl. Phys. Lett.* 95, 013106 (2009).
16. J.H. Lee, J.C. Grossman, J. Reed, and G. Galli, *Appl. Phys. Lett.* 91, 223110 (2007).
17. J.E. Ni, E.D. Case, K.N. Khabir, R.C. Stewart, C.I. Wu, T.P. Hogan, E.J. Timm, S.N. Girard, and M.G. Kanatzidis, *Mater. Sci. Eng. B* 170, 58 (2010).
18. B. Houston, R.E. Strakna, and H.S. Belson, *J. Appl. Phys.* 39, 3913 (1968).
19. N.G. Einspruch, R.J. Manning, and J. Acoust, *Soc. Am.* 35, 215 (1963).
20. J.R. Groza, S.H. Risbud, and K. Yamazaki, *J. Mater. Res.* 7, 2643 (1992).